A generic metric to quantify quorum sensing activation dynamics

Anand Pai[1,3], **Jaydeep K Srimani**[1], **Yu Tanouchi**[1], and **Lingchong You**[1,2,*]

[1]Department of Biomedical Engineering, Duke University, Durham NC 27708

[2]Institute for Genome Sciences and Policy, Duke University, Durham NC 27708

Abstract

Quorum sensing (QS) enables bacteria to sense and respond to changes in their population density. It plays a critical role in controlling different biological functions, including bioluminescence and bacterial virulence. It has also between widely adapted to program robust dynamics in one or multiple cellular populations. While QS systems across bacteria all appear to function similarly – as density-dependent control systems, there is tremendous diversity among these systems in terms of signaling components and network architectures. This diversity hampers efforts to quantify the general control properties of QS. For a specific QS module, it remains unclear how to most effectively characterize its regulatory properties, in a manner that allows quantitative predictions of the activation dynamics of the target gene. Using simple kinetic models, here we show that the dominant temporal dynamics of QS-controlled target activation can be captured by a generic metric, 'sensing potential', defined at a single time point. We validate these predictions using synthetic QS circuits in *Escherichia coli*. Our work provides a computational framework and experimental methodology to characterize diverse natural QS systems and provides a concise yet quantitative criterion for selecting or optimizing a QS system for synthetic biology applications.

Keywords

Synthetic circuits; quorum sensing; bacterial communication; signaling kinetics; sensing metric

Introduction

Quorum sensing (QS) is a communication mechanism by which bacteria sense and respond to changes in their density. The basic QS mechanism can be illustrated using the *lux* system of the bacterium *Vibrio fischeri* (Figure 1A). Within each cell of a QS population, an enzyme LuxI (S) synthesizes a signal molecule (acyl-homoserine lactone, or AHL) that diffuses across the cell membrane or is exported into the external environment (1, 2). At a low cell density, the signal concentration is low both inside and outside the cells. As the

*Corresponding author. you@duke.edu.
[3]Present address: Department of Biochemistry and Biophysics, University of California, San Francisco, CA 94158, Gladstone Institutes, San Francisco, CA 94158

density increases, the local signal concentration increases. Within the cells, a regulator protein LuxR (R), when bound to AHL, activates target gene expression. Therefore, target activation is correlated to local population density through the production and detection of the signal molecule.

Most bacteria appear to carry at least one QS system and many, such as *Vibrio harveyi* (3) and the human pathogen *Pseudomonas aeruginosa* (4), carry multiple systems. These QS systems across bacteria operate over a wide range of cell density and control a wide variety of target genes related to virulence, biofilm formation, enzyme secretion, and competence regulation (5, 6). QS systems display diverse architectures, a variety of signaling molecules and signal transport mechanisms, and employ different strategies to detect the signal (1). As a result of this diversity, there is no clear standard to quantify the density-dependent control characteristics of a QS system, which are often reported as a density range or the growth phase range in which the target appears to activate (7, 8). It is thus difficult to quantify the basic characteristics of a QS system, compare two QS systems, or measure how their characteristics are affected by genetic or environmental perturbations. Here, in place of the specifics of each QS systems, such as the architecture, signal molecules, or signal detection mechanism, we focus on the 'core' structure (Figure 1B) that is seen across QS systems and use it to examine how QS-mediated control can be quantified.

Results and discussion

Sensing potential as a reliable predictor of temporal QS dynamics

If we consider a QS system as a "black box", two properties are most critical in determining its regulation of a target gene: 1) its ability to gauge cell density from the dynamics of the QS signal; 2) response of the target gene to the QS signal. Given this notion, we hypothesized that a metric that integrates these two aspects would serve as an accurate predictor of QS activation dynamics. To this end, we have previously introduced the concept of "sensing potential" for a QS system. Mechanistically, it can be directly derived based on the specific reaction mechanism for each QS system (9). We note here that, by definition, sensing potential is determined by the cell density at a single time point, when the QS-mediated target gene is expressed at half maximum.

We wondered to what extent this metric could be used to predict the overall temporal dynamics of a QS system. To examine this question, we first modeled QS systems using the core module and its associated parameters (Figure 1B, Methods): signal synthesis (k), feedback (k_a), degradation (d_a), transport (D) and detection (K). We simulated density-dependent target activation ϕ (Figure 1C) over a wide range of parameter values; each parameter set here represented a distinct QS system. This technique, of computationally studying the characteristics of a variety of network based systems over a large parameter space (10–12), can provide insight into the common properties of diverse systems that are not apparent from studying each system in isolation.

In each simulation, we calculated the sensing potential as $v = \dfrac{1}{N_{\phi 50} V_c}$, where $N_{\phi 50}$ is the cell density for 50% activation of the target above any basal level of activation ϕ_{basal} and V_c

represents the cell volume (Figure 1C). In the same simulation, we then calculated the densities at which the target gene reaches 20%, 40%, 60%, and 80% of its maximum level. These activation levels and their corresponding densities together provide an overall representation of the density-dependent activation phenotype of the QS system, equivalent to the 'dose-response' shape of density versus the QS-regulated phenotype. We then examined the correlation between these measures with sensing potential.

These results (Figure 1D and Supplementary Figure 1A) demonstrated that the temporal profiles QS-mediated activation, as captured by the densities corresponding to varying activation levels (ϕ_{20}, ϕ_{40}, ϕ_{60}, ϕ_{80}), could indeed be predicted by the sensing potential (v). That is, even though v is defined at a single data point, it is highly predictive of the overall activation dynamics of a QS system. By definition of v, the prediction is perfect for 50% of QS activation (ϕ_{50}), corresponding to a straight line that lumps simulation results from all parameter combinations and different network motifs. For other activation levels, the corresponding densities also correlated monotonically with $1/v$, though the accuracy of prediction was lower (as indicated by the spread of data points) for activation levels further away from 50%.

We note that the ability of a single point in the density-dependent activation curve to predict the temporal characteristics is not specific to the use of 50% activation as threshold. The same behavior was observed if a different value such as 30% or 70% was used (Supplementary Figure 1B). Also, at the low values of v the densities corresponding to activation levels converge (top right corner in Figure 1D, see also Supplementary Figure 1A). This region captures QS systems that activate at high densities close to the carrying capacity. In these systems, the observed convergence is a combined result of the slow down of cell growth as density approaches carrying capacity and dynamics of signal accumulation – signal concentration at any given cell density increases and approaches its steady state value as cell growth slows down.

Importantly, as these simulations captured diverse QS systems, the results show that QS systems may be treated as a black box where their activation dynamics may be reliably quantified by v independent of the specifics of each system. Conversely, two QS systems can have the same v resulting from different parameters or architectures but would have largely the same phenotypic consequence for their respective hosts.

Experimental methodology to quantify QS-mediated activation

The above simulations suggest an approach to characterize diverse QS systems by direct phenotypic measurements: if we could determine such a metric for a given QS system, this value would allow us to determine the overall activation property of the QS system, without necessarily knowing the full mechanism of the underlying QS regulation or the corresponding parameters.

To this end, we sought to develop a general method to quantify QS in a high-throughput manner, by directly measuring the density-dependent target gene expression. As a well-defined model system, we used synthetic circuits in *E. coli* where circuit components are derived from the minimal components of a natural QS system; the well studied *luxR-luxI*

system from *V. fischeri* (13) (Figure 2A). The QS 'sensor' is represented by the plasmid pLuxRI where the genes *luxR* and *luxI* are under the control of lac/ara-1 promoter (14). In the *E. coli* cell strain MG1655, the lac/ara-1 promoter may be induced using IPTG but its repression is leaky (MG1655 does not overproduce the repressor LacI) and allows a low level promoter induction even in the absence of IPTG. The target of QS is on the plasmid pluxGFPuv, where reporter GFPuv expression is under control of the promoter P_{luxI} (15).

In each measurement, a high-density overnight culture of the QS cells (roughly 10^9 cells/ml) was strongly diluted (10^5 fold) into fresh medium and induced with 1mM IPTG. This low-density culture was then incubated in a plate reader using a 96-well plate (see Methods). Samples of the growing culture were periodically taken and analyzed by flow cytometry to obtain the reporter expression of individual cells in the population (Figure 2C). Following dilution, the average reporter expression by cells showed a characteristic 'U' shape; an initial decrease in reporter to the level where cells can be considered OFF for any reporter expression and later, an increase in reporter at high cell density (Figure 2C). This dynamics can be explained as follows: overnight grown cells were initially ON for reporter expression as they had earlier reached high density allowing for high signal accumulation. On dilution into fresh medium, intracellular and extracellular signal concentration reach low levels and reporter expression is no longer induced. Growth of these low-density cells dilutes the initial intracellular reporter concentration leading to a rapid decrease in reporter concentration in the first few hours of cell growth (QS OFF). Next, when the cell density becomes sufficiently high, the signal will reach sufficiently high levels to trigger reporter expression (QS ON region) (Figure 2C). This initial decrease and later increase in target expression with density is a well-known QS characteristic (16–18).

Alongside this periodic flow cytometry measurement, we also monitored the overall fluorescence level as well as the density (optical density (OD) at 600 nm) of the growing culture using a microplate reader (Figure 2D). This provided observations of the dynamics of QS activation with high temporal resolution (~every 10 minutes). The plate-reader measurements did not capture the earlier decrease (QS OFF region) following dilution. During that phase, the total fluorescence in each well was too low to be detected by the plate reader (Figure 2D). However, these measurements did accurately capture the QS-dependent activation (QS ON region). Thus, high-frequency measurement of the fluorescence and OD of the culture in the plate reader were used in all subsequent experiments to quantify target expression dynamics.

How do we quantify QS from these measurements? Often, the cell density corresponding to minimum in the U shaped reporter expression dynamics is used as a characteristic measure of the QS system (16). This provides a convenient way to characterize a given QS system as well as perturbations to it, including mutants in which different sections of the QS pathway have been deleted (16, 17). However, we found that this minimum point was sensitive to the initial cell density (Figure 3A). In addition, we noted that when starting from a low initial density, the population would reach and maintain an OFF state over a large range of density (Figure 2C) making the exact density at which minimum levels were reached difficult to accurately identify experimentally. Together, this made it difficult to develop the minimum point further as a reliable metric.

To eliminate this effect of initial density from our quantification of QS, we adopted a different approach. We noted that when diluted sufficiently strongly ($>10^3$ fold dilution of overnight culture), the observed QS-mediated activation on reaching high density, as observed from reporter expression, was independent of the initial density (Figure 3B). On starting growth from these high dilutions (low densities), all cultures first reach low (OFF) levels of reporter expression (Figure 2C). Then, QS-mediated activation of these cultures takes place on reaching a sufficient high density, as observed through the continuous increase in reporter expression with cell density (above the low background value). This activation profile is independent of initial density (Figure 3B). As such, it can serve as a much more reliable measure and we sought to quantify QS characteristics using this property.

To determine whether such a metric established based on a single point can experimentally capture temporal characteristics of QS activation, we first measured QS-mediated reporter production under various conditions using perturbations to the signal synthesis rate or the signal degradation rate. To control the signal synthesis rate we modulated the IPTG concentration which controls the rate of expression of the AHL-synthase LuxI,. Another method to modulate signal concentration is through a positive feedback on signal synthesis and is observed in several bacterial QS species (19–23). To study this, we incorporated positive feedback into our system by introducing an additional copy of the *luxI* gene under the PluxI promoter (Figure 2B). We observed that both increasing IPTG (Figure 4A) and introduction of feedback (Figure 4A inset) sped up QS activation. This result is consistent with expectation that faster signal synthesis rates lead to higher signal concentration at lower densities, in turn, leading to earlier QS activation (9).

We modulated signal degradation by changing the pH of the growth medium (24, 25). Irrespective of the starting pH, cell growth led to slight increase in the culture pH (Supplementary Figure 2A). However, this increase was uniform across all pH levels. Thus, changing the starting pH allowed us to reliably modulate signal degradation. At each pH level, we followed reporter production with cell-density (Figure 4B). We observed that QS-mediated activation decreased rapidly above pH 7. Using a constitutive GFP expression system, we confirmed that the decrease in reporter expression was not an indirect effect of pH on cellular physiology (Supplementary Figure 2B). This reduction with pH was consistent with experimental observations of increased AHL instability in alkaline media (24–27) and with theoretical predictions (9) that increasing signal degradation reduces the sensing potential.

If, as shown by our simulations (Figure 1D), a metric such as sensing potential calculated at a single point can predict the dynamics of activation, we expect measurements at any activation level ϕ to correlate with the critical density (ϕ_{50}) approximately. To examine this experimentally, we used the above QS-mediated reporter expression observations taking reporter dynamics to reflect QS-mediated activation (Figure 4 A, B, and Supplementary Figure 3). We set an arbitrary but sufficiently high (above basal) reporter level, and determined the critical density at which this threshold level is crossed. We then determined the corresponding activation densities at which reporter levels reached appropriate levels above (1.5 and 1.75 times) and below (0.5 and 0.75) this threshold. These activation

densities were then plotted against critical density across all the observations, keeping the threshold reporter level the same (see Supplementary Figure 3 for a detailed explanation of the quantification methodology).

We observed that despite the modulation in the critical density (horizontal spread of data points) and consistent with simulation results (Figure 1D and Supplementary Figure 1), activation densities correlated with critical density (Figure 4 C). Importantly, this correlation was inclusive of perturbations that changed both the kinetic parameters (pH, IPTG) and the architecture (through feedback) of QS regulation. The overlapping of points of the same activation level but representing distinct QS systems or conditions shows how a metric measured at a single point can still reliably capture the dominant activation properties of diverse QS systems. For example, the density dependent activation dynamics from the following QS modulations were similar: (1) QS cells in medium with pH 7 and low IPTG (0.25 mM) representing low signal degradation and production rate; (2) QS cells in medium with high pH (7.5) and high IPTG (1 mM), representing high signal degradation and production rate; (3) QS cells with signal feedback at pH 7 and no IPTG, representing low signal degradation with increased signal production through feedback (Figure 4C and Supplementary Figure 4). Together, these experimental results combined with simulations (Figure 1D) suggest that a single metric can capture and quantify the dominant characteristics of QS-mediated target-gene activation dynamics regardless of the specific details of the system.

The simulations and experiments show that quantifying QS using the sensing potential (v) can provide sufficient information to capture the dominant activation characteristics of a QS system, even if the underlying mechanism is more complex than the core module. Thus, v can be used as a single (reduced) metric to study how QS characteristics affect downstream regulation. We demonstrate that such a metric for a biological system can be estimated through the dynamics of target-function activation alongside cell density and may be particularly useful in measuring the effects of perturbations to a QS system and its environment (Figure 1D and 4). The ability of a single metric to capture activation dynamics in our experiments persisted through several complexities that would be expected with cell growth but were not explicitly accounted for in our simulations indicating the robustness of such quantification. These complexities include: non-monotonic cell growth rate variations not captured by simple logistic growth (see Supplementary Figure 3A); (2) the effect of reporter expression and IPTG on growth rate (3) the change in expression level of proteins with changes in growth rate (4) changes in cell size. We note here that our examination of the metric's abilities to capture QS dynamics was carried out using synthetic circuits, which account for many of the aforementioned biological complexities. However, natural QS systems would carry many additional complexities. It remains to be tested to what extent the metric captures the dynamics of natural QS systems. Furthermore, our results are based on well-mixed cultures where signal concentrations can assumed be uninform in each culture. For non-well-mixed systems, the spatial distribution of the bacterial population could lead to heterogeneity in local signal concentrations and hence, activation of a local population (28).

The metric and its mathematical framework also provide a quantitative link between the fundamental parameters and the QS phenotype and could hence provide a greater

understanding of the systems (29). Capturing the characteristics of a control system by a single metric could prove particularly beneficial in synthetic biology where QS is increasingly being used to engineer population level behavior (30, 31). Annotation of the diverse QS systems, available as parts for synthetic circuits, for their v's would provide a catalog for circuit design (32). A desired v can then be used as selection criteria for expected function control.

Materials and methods

Mathematical modeling diverse QS systems

For each QS system, we built a minimal model using ordinary differential equations for the intracellular and extracellular signal concentrations depending on the system architecture. A more detailed analysis of this model formulation was done in ref. (9) described as a Type II QS system where intracellular signal concentration is detected by cytoplasmic regulators and signal diffuses freely in and out of the cell. Consider the system in Figure 1A for a single cell in a population of cell density N. The rate of change of the intracellular and extracellular signal respectively is given by:

$$\frac{dA_i}{dt} = k + k_a A_i - D(A_i - A_e) - d_a A_i, \quad \text{A1}$$

$$\frac{dA_e}{dt} = D(A_i - A_e)\left(\frac{V_c}{V_e}\right) - d_a A_e, \quad \text{A2}$$

where

A_i and A_e represent intracellular and extracellular signal concentrations;

k denotes basal signal synthesis rate;

$D(A_i - A_e)$ accounts for diffusion of the signal to the culture;

$k_a A_i$ accounts for the signal synthesis by positive feedback.

V_c denotes the average cell volume;

V_e denotes the average volume of a the microenvironment for each cell $(V_e = {}^1\!/_N)$;

d_a denotes the degradation rate constant of the signal (inside or outside the cell).

We assume that V_c remains constant during population growth. We further assume that intracellular signal A_i-based target activation ϕ follows Hill kinetics (15, 32) with cooperativity a where $1 < a < 2$. We chose $a = 1.6$

$$\phi = \frac{A_i^a}{K^a + A_i^a} \quad \text{A3}$$

Here K represents the half-maximal concentration for target activation.

Alongside signaling dynamics, cell growth is modeled by a logistic equation

$$\left(\frac{dN}{dt}\right) = gN\left(1 - \frac{N}{N_m}\right), \quad \text{A4}$$

with N_m as carrying capacity and g the specific growth rate.

Note 1: In eq. A1 where A_e is zero (such as when cell density is very small and thus $N \to 0$) the steady state A_i is then given by $A_{i,ss} = k \big/ (D+d_a)$. This shows that for any positive, finite values of the fundamental parameters, $A_{i,ss}$ is always greater than zero. In other words, a low basal level of signal always exists inside cells as long as there is some signal production and either signal diffusion or degradation is not infinitely large (typically $D \gg d_a$). The basal level of target activation ϕ_{basal} corresponding to this signal level can be calculated as $\phi_{basal} = \dfrac{A_{i,ss}{}^a}{K^a + A_{i,ss}{}^a}$. This activation by the basal signal level can lead to non-zero activation levels irrespective of density (33). However, this activation by basal intracellular signal is not encountered in QS systems where extracellular signal A_e mediates QS response. Thus, to unify QS system types irrespective of the level of basal activation, we redefine the activation level as

$$\phi = \phi_{basal} + (1 - \phi_{basal})\phi_{QS} \quad \text{A5}$$

Thus v is calculated from the density $N_{\phi 50}$ at which $\phi50 = \phi_{basal} + (1-\phi_{basal})0.5$ (Figure 1C). Similarly, the dynamic characteristics are the densities $N_{\phi x}$ at which $\phi_x = \phi_{basal} + (1-\phi_{basal})x$, where x is the activation under density-dependent control (plotted in Figure 1D)

Note 2: For simplicity, we assume that the signal degradation rate constant (d_a) is the same in the intracellular and extracellular compartments. It may in fact be different in these compartments: cell-growth induced dilution would act in the intracellular compartment, whereas changes in the culture pH would likely impact the extracellular degradation more strongly. However, due to fast signal diffusion between the two compartments and the large size of V_e in comparison to V_c (even at high cell densities $V_e \gg V_c$), degradation in the extracellular compartment acts as the major signal sink and thus as the major determinant of signal concentration by degradation (for both A_i and A_e, see Supplementary Figure 5). Thus the parameter d_a can be interpreted to be the signal degradation rate constant in the extracellular compartment.

Parameters d_a, D, k, k_a, K for each QS system, were chosen randomly within the bounds shown below. For each set of parameters, equations A1–A5 were simulated starting from a low density 10^5 cells/ml. v for a system was determined as described in the text at the density for 50% activation above basal activation as described by eq. A5 and shown in Figure 1C. Bounds for the parameter values were based on earlier estimations of natural QS system parameters (9). The following parameter bounds were used for QS with feedback: $k = 2 - 5 \times 10^3$ nM hr^{-1}, $k_a = 1 - 50$ $D = 1 - 4 \times 10^2$ hr^{-1}, da $= 0.01 - 0.1$ hr^{-1}, $K = 10 - 50$nm. To separately capture QS systems without feedback, a larger range of k ($k = 1 - 10 \times 10^3$) nM hr^{-1} was used so as to achieve a similar spread of sensing potential values covered with both architectures. 500 simulations of randomly chosen parameter sets were

carried out for each case: QS with and without feedback. Results from all parameter sets for which QS-mediated activation reached at least the activation levels that we chose to mark v (50% in Figure 1D, 30% and 70% in Supplementary Figure 1B) by the end of growth were plotted.

Strains, media and growth conditions—MG1655 cells were used throughout this study. Unless mentioned otherwise, pH-buffered TBK medium (10 g tryptone, 7 g KCl per litre buffered with 100mM MOPS) at 30°C was used. Cells were first grown overnight from single colonies in duplicate in the presence of appropriate antibiotics in 3ml cultures grown in 14ml tubes in shaker incubator at 30°C. In the morning, 1 ml of cell culture was washed twice with distilled water and diluted 10^5 fold (or as indicated in Figure 4A, B). 200 μl of culture with desired IPTG and pH level was added to 96 well black plates. 50μl of mineral oil was added to prevent evaporation and the plate was incubated in plate reader (Victor3, Perkin-Elmer) at 30°C. Readings of OD (Absorbance 600 nm) and GFP (using filters for excitation at 405 nm, emission at 535 nm) were taken every 10 minutes with periodic shaking (5s orbital). Correlation between OD measured in the plate reader and cell density was taken to be linear (32, 34, 35). This combination of media and conditions provided appropriate low growth rate and low background for the detection of GFP signal in plate reader. For flow cytometry reading, 20 replicate wells of the appropriate cell culture (pLuxR or pLuxRI plasmid with pluxGFPuv) were grown in a plate as above. Periodically, 100–200μl from an unsampled well was removed and mixed with 500 μl water. Cells were then spun down and resuspended in 1% formaldehyde for fixing. Samples were analyzed by flow cytometry using a FACSCantoII (BD Biosciences) within 2 days of fixation (488 nm excitation, 530 nm emission, FITC pulse height). For exogenous AHL dilution, $3OC_6AHL$ (Sigma) was first dissolved in ethyl acetate as the stock solution (20 mM). For use, 5 μl of this solution was taken in a 1ml centrifuge tube and the ethyl acetate was evaporated under a column of air. 995 μl of TBK media with appropriate antibiotics was added to make 100 μM solution which can be used as 1000 nM when diluted 100 fold into a well.

Processing plate-reader data—The high throughput data from the plate reader is in the form of time, OD, and reporter expression level (Supplementary Figure 3). Reporter expression data was normalized against OD_{600} to provide reporter expression per cell. Normalized GFP expression was calculated by subtracting GFP reading of blank TBK and dividing by corresponding OD_{600} subtracted for blank TBK. Normalized data was denoised in MATLAB using a local regression. To calculate critical density at which threshold reporter level is crossed, an activation OD range was selected and the corresponding normalized GFP data were fit with a third order polynomial (bounded within a region of interest of reporter values), to avoid non-monotonic fluctuations in plate reader data. A threshold reporter expression level corresponding to ϕ_{50}, was selected (4000 a.u of normalized GFP expression), and the densities at which higher and lower levels were reached were determined by interpolating directly or based on a fitted polynomial (marked as $\phi_{0.25}$, $\phi_{0.5}$, $\phi_{1.5}$, $\phi_{1.75}$ for reaching 0.25, 0.5, 1.5 and 1.75 times the threshold level). Supplementary Figure 3 shows this methodology applied to a sample observation of QS-mediated activation.

Supplementary Material

Refer to Web version on PubMed Central for supplementary material.

Acknowledgments

References

1. Ng WL, Bassler BL. Bacterial quorum-sensing network architectures. Annu Rev Genet. 2009; 43:197–222. [PubMed: 19686078]

2. Williams P, Winzer K, Chan WC, Camara M. Look who's talking: communication and quorum sensing in the bacterial world. Philos Trans R Soc Lond B Biol Sci. 2007; 362(1483):1119–1134. [PubMed: 17360280]

3. Long T, et al. Quantifying the integration of quorum-sensing signals with single-cell resolution. PLoS Biol. 2009; 7(3):e68. [PubMed: 19320539]

4. Schuster M, Greenberg EP. A network of networks: quorum-sensing gene regulation in Pseudomonas aeruginosa. Int J Med Microbiol. 2006; 2962(2-3):73–81. [PubMed: 16476569]

5. Gonzalez JE, Marketon MM. Quorum sensing in nitrogen-fixing rhizobia. Microbiol Mol Biol Rev. 2003; 67(4):574–592. [PubMed: 14665677]

6. Smith RS, Iglewski BH. P. aeruginosa quorum-sensing systems and virulence. Curr Opin Microbiol. 2003; 6(1):56–60. [PubMed: 12615220]

7. Lupp C, Urbanowski M, Greenberg EP, Ruby EG. The Vibrio fischeri quorum-sensing systems ain and lux sequentially induce luminescence gene expression and are important for persistence in the squid host. Molecular microbiology. 2003; 50(1):319–331. [PubMed: 14507383]

8. Pesci EC, Pearson JP, Seed PC, Iglewski BH. Regulation of las and rhl quorum sensing in Pseudomonas aeruginosa. Journal of bacteriology. 1997; 179(10):3127–3132. [PubMed: 9150205]

9. Pai A, You L. Optimal tuning of bacterial sensing potential. Mol Syst Biol. 2009; 5:286. [PubMed: 19584835]

10. Brandman O, Ferrell JE Jr, Li R, Meyer T. Interlinked fast and slow positive feedback loops drive reliable cell decisions. Science. 2005; 310(5747):496–498. [PubMed: 16239477]

11. Ma W, Trusina A, El-Samad H, Lim WA, Tang C. Defining network topologies that can achieve biochemical adaptation. Cell. 2009; 138(4):760–773. [PubMed: 19703401]

12. Tsai TY, et al. Robust, tunable biological oscillations from interlinked positive and negative feedback loops. Science. 2008; 321(5885):126–129. [PubMed: 18599789]

13. Fuqua C, Greenberg EP. Listening in on bacteria: acyl-homoserine lactone signalling. Nat Rev Mol Cell Biol. 2002; 3(9):685–695. [PubMed: 12209128]

14. Lutz R, Bujard H. Independent and tight regulation of transcriptional units in Escherichia coli via the LacR/O, the TetR/O and AraC/I1-I2 regulatory elements. Nucleic Acids Res. 1997; 25(6): 1203–1210. [PubMed: 9092630]

15. Collins CH, Arnold FH, Leadbetter JR. Directed evolution of Vibrio fischeri LuxR for increased sensitivity to a broad spectrum of acyl-homoserine lactones. Mol Microbiol. 2005; 55(3):712–723. [PubMed: 15660998]

16. Henke JM, Bassler BL. Three parallel quorum-sensing systems regulate gene expression in *Vibrio harveyi*. J Bacteriol. 2004; 186(20):6902–6914. [PubMed: 15466044]

17. Miller MB, Skorupski K, Lenz DH, Taylor RK, Bassler BL. Parallel quorum sensing systems converge to regulate virulence in Vibrio cholerae. Cell. 2002; 110(3):303–314. [PubMed: 12176318]

18. Lenz DH, Bassler BL. The small nucleoid protein Fis is involved in Vibrio cholerae quorum sensing. Molecular microbiology. 2007; 63(3):859–871. [PubMed: 17181781]

19. Morrison DA, Lee MS. Regulation of competence for genetic transformation in Streptococcus pneumoniae: a link between quorum sensing and DNA processing genes. Research in microbiology. 2000; 151(6):445–451. [PubMed: 10961457]

20. Waters CM, Bassler BL. Quorum sensing: cell-to-cell communication in bacteria. Annual review of cell and developmental biology. 2005; 21:319–346.

21. Li YH, Lau PC, Lee JH, Ellen RP, Cvitkovitch DG. Natural genetic transformation of Streptococcus mutans growing in biofilms. Journal of bacteriology. 2001; 183(3):897–908. [PubMed: 11208787]

22. Lithgow JK, et al. The regulatory locus cinRI in Rhizobium leguminosarum controls a network of quorum-sensing loci. Molecular microbiology. 2000; 37(1):81–97. [PubMed: 10931307]

23. Bartels FW, et al. Effector-stimulated single molecule protein-DNA interactions of a quorum-sensing system in Sinorhizobium meliloti. Biophysical journal. 2007; 92(12):4391–4400. [PubMed: 17384071]

24. Kaufmann GF, et al. Revisiting quorum sensing: Discovery of additional chemical and biological functions for 3-oxo-N-acylhomoserine lactones. Proc Natl Acad Sci U S A. 2005; 102(2):309–314. [PubMed: 15623555]

25. Yates EA, et al. N-acylhomoserine lactones undergo lactonolysis in a pH-, temperature-, and acyl chain length-dependent manner during growth of Yersinia pseudotuberculosis and Pseudomonas aeruginosa. Infect Immun. 2002; 70(10):5635–5646. [PubMed: 12228292]

26. Schaefer AL, Hanzelka BL, Parsek MR, Greenberg EP. Detection, purification, and structural elucidation of the acylhomoserine lactone inducer of Vibrio fischeri luminescence and other related molecules. Methods Enzymol. 2000; 305:288–301. [PubMed: 10812608]

27. Horswill AR, Stoodley P, Stewart PS, Parsek MR. The effect of the chemical, biological, and physical environment on quorum sensing in structured microbial communities. Anal Bioanal Chem. 2007; 387(2):371–380. [PubMed: 17047948]

28. Hense BA, et al. Does efficiency sensing unify diffusion and quorum sensing? Nat Rev Microbiol. 2007; 5(3):230–239. [PubMed: 17304251]

29. Phillips R, Milo R. A feeling for the numbers in biology. Proc Natl Acad Sci U S A. 2009; 106(51):21465–21471. [PubMed: 20018695]

30. Xavier JB. Social interaction in synthetic and natural microbial communities. Mol Syst Biol. 2011; 7:483. [PubMed: 21487402]

31. Pai A, Tanouchi Y, Collins CH, You L. Engineering multicellular systems by cell–cell communication. Curr Opin Biotechnol. 2009

32. Canton B, Labno A, Endy D. Refinement and standardization of synthetic biological parts and devices. Nat Biotechnol. 2008; 26(7):787–793. [PubMed: 18612302]

33. Pai A, Tanouchi Y, You L. Optimality and robustness in quorum sensing (QS)-mediated regulation of a costly public good enzyme. Proc Natl Acad Sci U S A. 2012; 109(48):19810–19815. [PubMed: 23144221]

34. Dekel E, Alon U. Optimality and evolutionary tuning of the expression level of a protein. Nature. 2005; 436(7050):588–592. [PubMed: 16049495]

35. Koch AL. Turbidity measurements of bacterial cultures in some available commercial instruments. Anal Biochem. 1970; 38(1):252–259. [PubMed: 4920662]
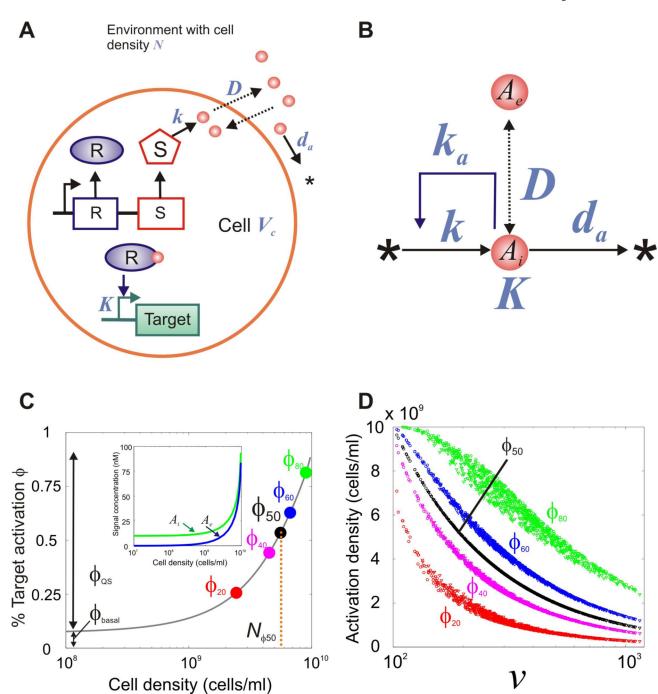
Figure 1. Predicting quorum sensing-mediated target activation by sensing potential

(A) QS by a single cell of volume V_c in a population of density N. Signal (red dots) is produced intracellularly by synthase S and diffuses freely across the cell which senses the intracellular concentration using detector R for target activation. Rate constants for signal synthesis (k), transport by diffusion (D) and signal degradation (d_a) and threshold signal concentration (K) are indicated.

(B) Minimal network-based representation of QS showing only signaling dynamics in terms of production, transport and degradation. Green box shows the simplified representation of the system in Figure 1A. Red filled circle indicate intracellular (A_i) or extracellular (A_e) signal. Dotted red box denotes detection of intracellular signal concentration for target activation.

Arrows indicate the synthesis of a signal from cellular substrates, the transport of signal between the cell and the environment, and the degradation of the signal. For simplicity, degradation of signal in the environment is not shown. Relevant rate constants described in text are indicated next to the arrows.

(C) Under QS control, as cell density increases, so does target gene activation ϕ. Dynamics of signal production and transport causes a minimum basal activation level within the cells irrespective of cell density (see Methods) and is marked as ϕ_{basal}. Density-dependent activation above this level is marked as ϕ_{QS}. The cell density $N_{\phi 50}$ at which the target is half-maximal of ϕ_{QS} is used to estimate v (black dot). Colored circles mark the points where the other activations levels (20%, 40%, 60% and 80% of ϕ_{QS} are reached). Inset: Intracellular and extracellular signal concentration during population growth. Note the basal level of intracellular signal.

(D) Temporal properties of QS systems can be predicted by their v. Each dot corresponds to the results from one parameter set for a chosen QS type. 1000 different parameter sets were randomly generated for the simulations. Despite the diversity of QS systems generated, the dynamic characteristics ϕ_{20}, ϕ_{40}, ϕ_{60}, ϕ_{80} correlate strongly with v as a metric and largely collapse to the same line for each activation level. By definition of v, the data points for ϕ_{50} (black dots) must lie on the same curve.
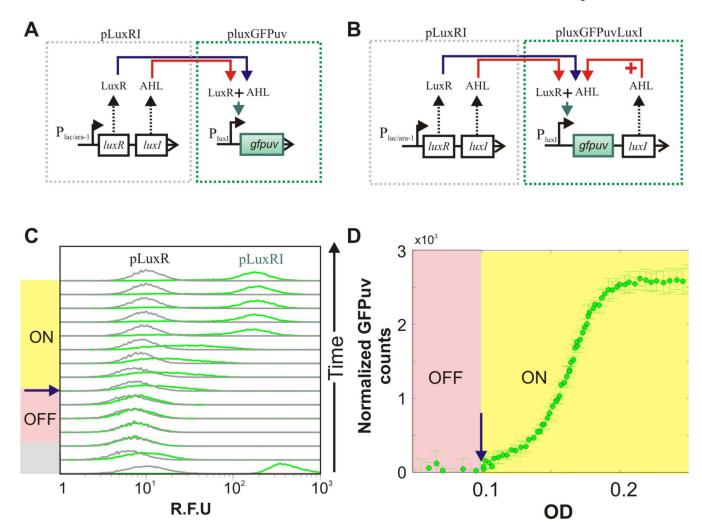
Figure 2. Quantifying QS activation in synthetic gene circuits

(A) The QS genes are carried by pLuxRI plasmid where LuxR and LuxI are under IPTG control (in LacI+ strains). pluxGFPuv acts as the reporter for QS wherein the GFP variant GFPuv is produced under the control of the P_{LuxI} promoter.

(B) QS circuit with feedback on signal synthase *luxI*.

(C) MG1655 cells grown in TBK media with 1mM IPTG at 30°C were observed periodically using flow cytometry for GFP expression. Cells carried either pLuxRI and pluxGFPuv (green:QS) or pLuxR and pluxGFPuv (grey) as luxI negative control. The histogram of GFP fluorescence at different time points after dilution starting from the overnight culture is shown. QS controlled fluorescence initially decreases to the same level as control cells but starts to increase again at high density (OD > 0.1). Shaded rectangles on the left mark regions where fluorescence decreases (pink), stays low or OFF (grey) and increases (yellow).

(D) Continuous high throughput monitoring of culture density (OD) and culture fluorescence (normalized to OD) in plate reader alongside the flow measurement in B shows the QS controlled transition from OFF (grey region) to ON (yellow shaded region). Blue arrow marks the corresponding point (by OD measurement) at which GFP expression was visible by flow measurement in B. The initial decrease seen in flow measurement in B (grey) is not visible here since initial dilution density is below OD based detection. The transition from OFF to ON takes place in the same OD range as observed with flow cytometry. Colored circles depict the mean values while error bars are the standard deviation measured from three technical replicates.
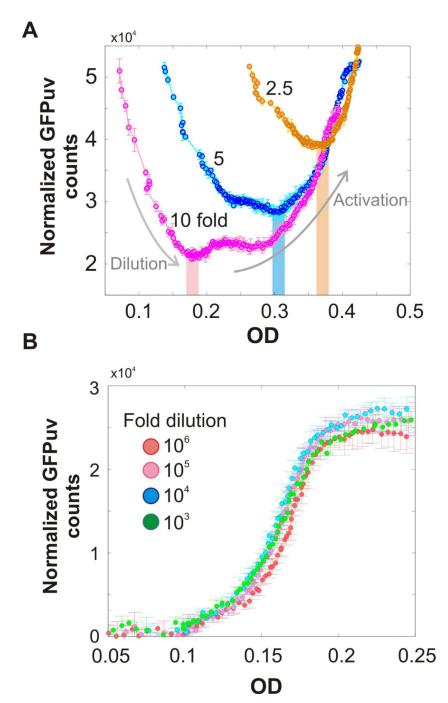
Figure 3. Quantifying QS characteristics independent of initial conditions

For all the dilutions, cells were grown under the same conditions (TBK media, 30°C with 1mM IPTG and appropriate antibiotics) but diluted to different initial densities as indicated.

(A) At higher initial cell densities (by lower dilutions of the overnight cultures), characteristic U shaped dynamics were observed but the position of the dynamics as well as features such as the critical density (vertical shaded rectangles) depended on the initial density.

(B) At lower initial cell densities (by higher dilutions of the overnight cultures), the density dependent reporter expression observed was independent of initial densities - the curves for the different indicated dilutions overlap. Values shown indicate

dilution level of overnight culture. Colored circles depict the mean values while error bars are the standard deviation measured from three technical replicates.
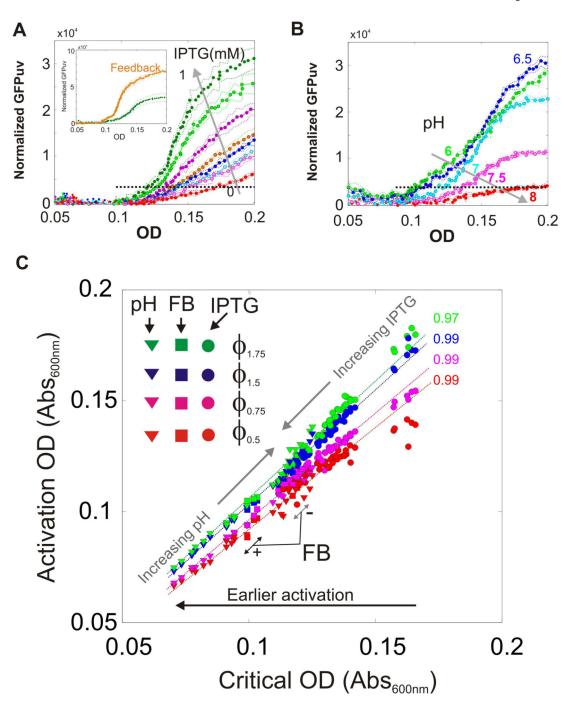
Figure 4. Sensing potential predicts temporal characteristics of QS activation under perturbed conditions
(A) Density dependent reporter expression from cells grown in media buffered to pH 7.0 under the different IPTG levels indicated. Inset: Comparison of cells carrying the positive feedback circuitry against the earlier case without feedback, both at 1mM IPTG.
(B) Density-dependent reporter expression from cells grown with 1mM IPTG under different pH conditions. Colored circles depict the mean values while the dotted lines of corresponding color indicate the standard deviation measured from three technical replicates.

(C) Temporal characteristics of QS-mediated activation can be predicted by critical density. For example, points corresponding to $\phi_{0.5}$ mark density (on y-axis) where reporter levels reached 50% of threshold value (4000 a.u) plotted against the critical density at which threshold density was reached (on x-axis). Data points are obtained from the IPTG, pH, and feedback based modulation of QS (3 replicates each for two clones for each condition). In addition to points described by the legend, data from feedback system (FB) in the presence and absence of IPTG are indicated for clarity: double headed arrows indicate approximate region where the points cluster (+/− indicate presence/absence of IPTG). Note that IPTG and FB modulations were carried out at pH 7. Conversely, pH modulations were carried out at IPTG 1mM. Supplementary Figure 3 shows additional details on this quantification methodology. Lines indicate linear fit for each activation level; correlation coefficient R for each activation level (against critical density) is indicated at the end of each line. All correlation values were significant (P<<0.01)